Journal of Medicinal Chemistry

ARTICLE

pubs.acs.org/jmc

Phase Transitions in Oleic Acid and in Human Breast Tissue As Studied by Raman Spectroscopy and Raman Imaging

Beata Brozek-Pluska,[†] Joanna Jablonska-Gajewicz,[‡] Radzislaw Kordek,[‡] and Halina Abramczyk*[,†]

[†]Laboratory of Laser Molecular Spectroscopy, Institute of Applied Radiation Chemistry, Technical University of Lodz, Wroblewskiego 15, 93-590 Lodz, Poland

[‡]Department of Pathology, Chair of Oncology, Medical University of Lodz, Paderewskiego 4, 93-509 Lodz, Poland

ABSTRACT: We present the results of differential scanning calorimetry (DSC) and Raman studies in the temperature range of 293−77 K on vibrational properties of the oleic acid and the human breast tissue as a function of temperature. We have found that vibrational properties are very sensitive indicators to specify phases and phase transitions at the molecular level. We have found that water content confined in the cancerous tissue is markedly different from that in the noncancerous tissue. The OH stretching vibrations of water are useful as potential Raman biomarkers to distinguish between the cancerous and the noncancerous human breast tissues. Our results provide experimental evidence on the role of lipid profile and cell hydration as factors of particular significance in differentiation of the noncancerous and cancerous breast tissues.

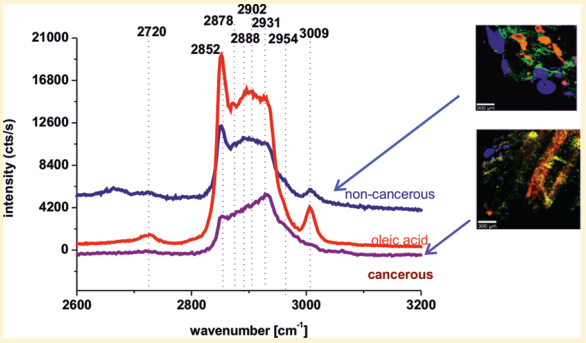

INTRODUCTION

There are many papers[1] reporting that dietary monounsaturated fatty acids appear to be protective against breast cancer. The recent papers have stimulated renewed interest in oleic acid. The recent discovery[2] demonstrates that the oleic acid significantly down-regulates the expression of some the most important oncogenes in breast cancer, cutting human epidermal growth factor receptor 2 (Her-2/neu) by up to 46%. In addition, it also boosts the effectiveness of Herceptin-based immunotherapy by promoting the death of breast cancer cells exhibiting high levels of the oncogene. On the other hand, there are studies that have reported that oleic acid may promote breast cancer.[3,4] On the basis of a number of spectroscopic and other physical methods (DSC, density, viscosity, self-diffusion), it has been suggested[5−7] that oleic acid has a quasismectic liquid crystal structure in the temperature range from the melting at 15 °C to about 30 °C. The structure between 30 and 55 °C consists of clusters with a less ordered structure, while the structure above 55 °C appears to be an isotropic liquid. Below the melting temperature the oleic acid exists in three solid state phases: α, β, γ. They have been identified by X-ray diffraction,[8−10] vibrational spectroscopy,[11−14] and differential scanning calorimetry.[15] It has been found that the α−γ transition occurs at −2.2 °C and represents a disorder−order transition, where in the α phase, the alkyl chain on the methyl side of the C═C bond exhibits conformational disorder, while the segment on the carboxyl side of C═C bond remains in the ordered all-trans conformation. The γ phase represents more ordered structure, in which the unit cell is pseudo-orthorhombic (space group $P21 = a$) with four molecules (or two hydrogen bonded dimers) per unit cell. The molecules are bent at the C═C bond, and the hydrocarbon chains pack according to the orthorhombic $O_{\parallel}'$ subcell (space group $Pma2$).[8−10]

The three oleic acid solid state polymorphs (α, β, and γ) have also been identified on the basis of pressure studies on thermal transitions of oleic acid polymorphs by high-pressure differential thermal analysis.[15,16] The β phase exists in two modifications: stable $\beta 1$ and metastable $\beta 2$. In the $\beta 1$ phase the unit cell belongs to a triclinic system of $P1$ where the asymmetric unit contains two crystallographically independent molecules A and B. The molecular layer exhibits a unique interdigitated structure, where the methyl group of molecule A and the carboxyl group of molecule B are located in the same plane. The methyl- and the carboxyl-sided chains together form a $T_{\parallel}$ subcell. The β phase is unique, has been found only in oleic acid, and does not show an order−disorder type solid-state transition.[8,9]

The goal of the paper is to explore phase transitions of oleic acid in the pure state and in human breast tissue in a broad range of temperatures, 77−293 K. In the paper presented here, Raman spectroscopy in the range 293−77 K was employed to investigate whether or not oleic acid exists in a separate phase within breast tissue lipids. The results should not only help in understanding the molecular mechanisms by which individual dietary fatty acids regulate the normal and malignant behavior of breast cancer cells in the tissue but also offer suggestions for the molecular mechanisms which drive the transformation of normal human cells into highly malignant derivatives.

Received: February 17, 2011
Published: April 08, 2011

RESULTS AND DISCUSSION

Figure 1 presents the DSC thermogram of oleic acid. The sample exhibits endothermic transitions at 267 and 282 K and exothermic transitions at 262 and 275K.

Figure 2a shows the Raman spectra of the oleic acid in the pure state and the Raman spectra of the normal (noncancerous) and cancerous human breast tissues in the region of 2600−3200 cm^{-1} at 293 K. Detailed analysis of Figure 2a demonstrates that there are many similarities in the lipid profile of the oleic acid and that of the normal breast tissue in contrast to the cancerous tissue.

In order to rationalize the vibrational features of the cancer pathology in localized regions observed in the Raman images (Figure 2b and Figure 2c), we have employed principal component analysis (PCA) method to analyze various areas of the noncancerous and cancerous breast tissues. The detailed discussion is beyond the scope of the paper, but the main conclusions are the following. We have found that the Raman spectra of the normal breast tissue in the blue regions are almost identical to those observed in the monounsaturated oleic acid that is a common constituent of glycerides. Thus, we have assigned the blue areas of the Raman images to adipose tissue. Detailed analysis of Raman images in Figure 2b and Figure 2c of the normal and cancerous breast tissues demonstrates that the normal tissue has evidently higher content of the adipose tissue than the cancerous tissue (much more blue areas).

The orange areas have the identical lipid profile as the blue areas but higher content of carotenoids. The green areas in the form of apparent wires in the normal breast tissue and yellow islands in the cancerous tissue represent the regions of non-identified chromophores, which exhibit strong autofluorescence (when excited with 532 nm). The most dominant breast tissue fluorophores are most likely tryptophane and flavoproteins.[17]

The red areas in the cancerous breast tissue represent regions rich in water, lipids, and proteins without any carotenoids. In contrast to the normal tissue, the Raman lipid pattern in the cancerous tissue does not resemble the composition of lipids in the adipose tissue (triglycerides) or the epithelium.

To summarize, a comparison between the Raman images of the noncancerous tissue and the cancerous tissue demonstrates that the normal tissue contains a markedly higher amount of fatty adipose cells, which strongly suggests that the presence of the adipose tissue may be inversely related to breast cancer risk. This observation, analyzed in the context of a number of references,[1,2] suggests that fatty acids and products of their metabolism play an important role in molecular mechanisms of carcinogenesis.

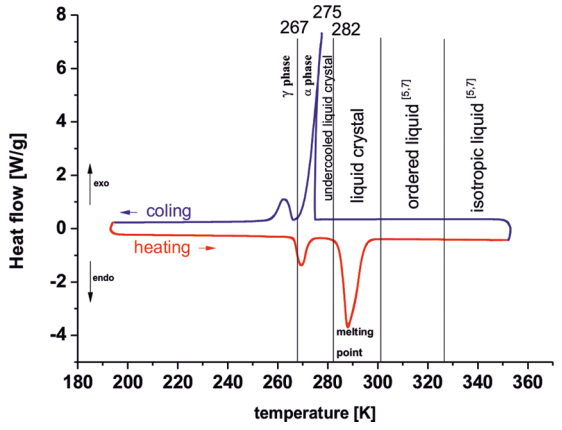

Figure 1. DSC thermogram of oleic acid.

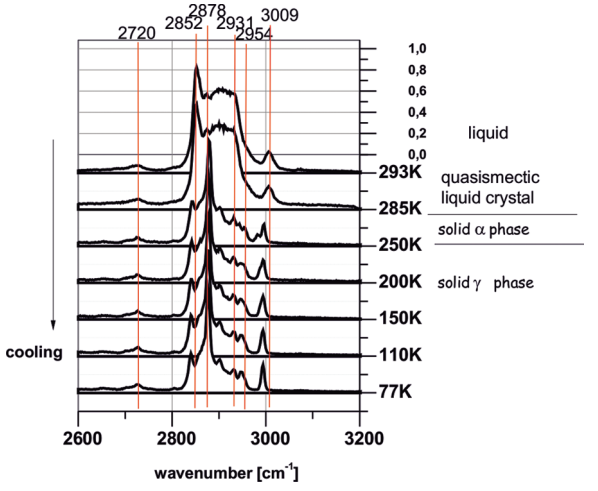

Figure 3. Raman spectra in the region of 2600−3200 cm^{-1} of oleic acid in the pure state over the temperature range of 77−293 K.

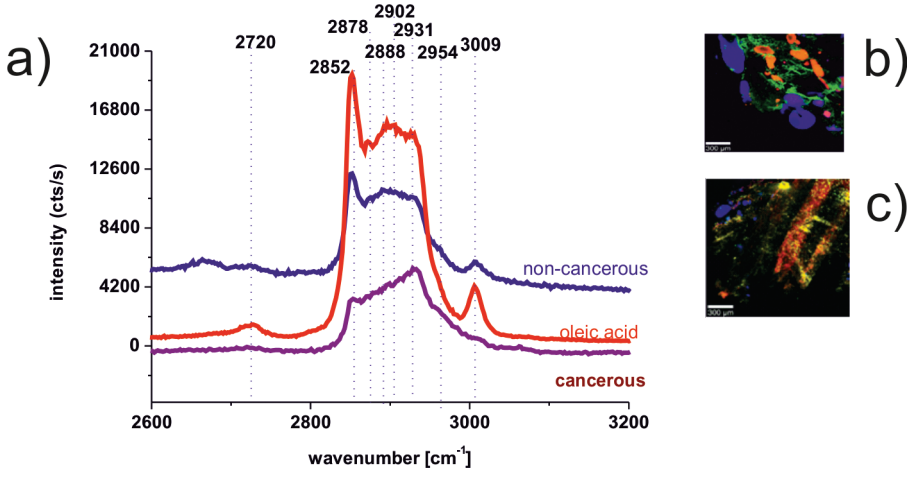

Figure 2. Raman spectra of the oleic acid in the pure state and of the human breast tissue in the region of 2600−3200 cm^{-1} at 293 K (a). Raman images of the human breast tissue: noncancerous (b); cancerous (infiltrating ductal carcinoma) (c).

dx.doi.org/10.1021/jm200180f |J. Med. Chem. 2011, 54, 3386–3392

It is interesting to examine if the oleic acid contained within the endogenous human breast tissue lipids exists in a separate phase. To answer this question, we have recorded the Raman spectra of the breast tissue and the oleic acid in the pure state over a broad temperature range of 293−77 K.

The spectra of the C−H vibrations of the hydrocarbon chains are sensitive to the conformational changes, mobility, and disorder−order transitions and usually exhibit distinct temperature induced changes. This indeed happens for the oleic acid. The various changes in the Raman spectra are presented in details in Figure 3 and Figure 4.

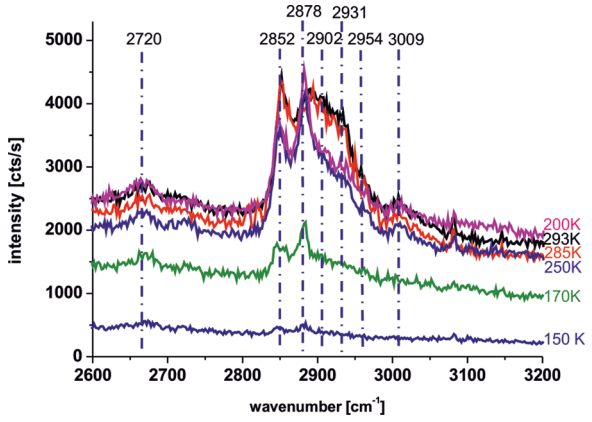

Figure 4. Raman spectra of the human breast tissue in the region of 2600−3200 cm^{-1} over the temperature range of 293−150 K.

Figure 3 shows the Raman spectra in the region of 2600−3200 cm^{-1} of the oleic acid in the pure state over a temperature range of 77−293 K. The bands at 2852, 2878, 2931, 2954 cm^{-1} are assigned to symmetric and asymmetric C−H stretching modes. The band 3009 cm^{-1} is assigned to the C−H stretching mode at the unsaturated bond of the hydrocarbon chain H−C═C. The detailed assignments of the major bands are presented in Table 1.

Figure 4 shows the Raman spectra of the human breast tissue in the region of 2600−3200 cm^{-1} over a temperature range of 150−293 K.

The comparison between Figure 3 and Figure 4 demonstrates that there are many similarities in temperature dependence of the lipid profile of the oleic acid in the pure state and the lipid profile of the normal breast tissue.

The valuable conclusions regarding the liquid structure and the phase transitions can be reached from the temperature dependences of the maximum peak positions. Figure 5 shows the temperature dependence of the maximum peak positions for the vibrations in the region of 2600−3200 cm^{-1}. As shown in Figure 5, the temperature responses of the maximum peak positions of the C−H stretching modes clearly reveal the abrupt shifts at 285 and 270 K that we have assigned to the phase

Table 1. Assignments of the Major Bands for Raman Spectra of Normal (Noncancerous) and Cancerous Human Breast Tissues and Various Phases of the Oleic Acid[30,31]

		major assignment			peak position [cm^{-1}]			major assignment	
no.	peak position [cm^{-1}]				γ (at 250 K)	α (at 271 K)	melt (at 293 K)		
1	2852	saturated bonds of lipids	CH_2	symmetric stretching mode	2847	2849	2852	cooling	CH_2
					2848	2848.7	2852	heating	symmetric stretching mode
2	2888	saturated bonds of lipids	$(CH_2)C-H$	asymmetric stretching mode	2878	2880	2871	cooling	$(CH_2)C-H$
					2878	2880	2871	heating	asymmetric stretching mode
3	2902	saturated bonds of lipids	$\nu(CH_2)$	stretching mode methyl - sided chain	2903	2903	2894	cooling	$\nu(CH_2)$
					2903	2903	2894	heating	stretching mode methyl-sided chain
4	2931	saturated bonds of lipids	CH_2	asymmetric stretching mode	2933	2932	2912	cooling	CH_2
					2932	2931	2912	heating	asymmetric stretching mode
5	2954	saturated bonds of lipids	CH_3	asymmetric stretching mode	2954	2971	2933	cooling	CH_3
					2955	2962	2933	heating	asymmetric stretching mode
6	3009	unsaturated bonds of lipids	H−C═C	stretching mode	2994	3004	3007	cooling	H−C═C
					2994	3002	3007	heating	stretching mode
7	3240	water	OH	stretching mode					
8	3390	water	OH	stretching mode					

dx.doi.org/10.1021/jm200180f |J. Med. Chem. 2011, 54, 3386–3392

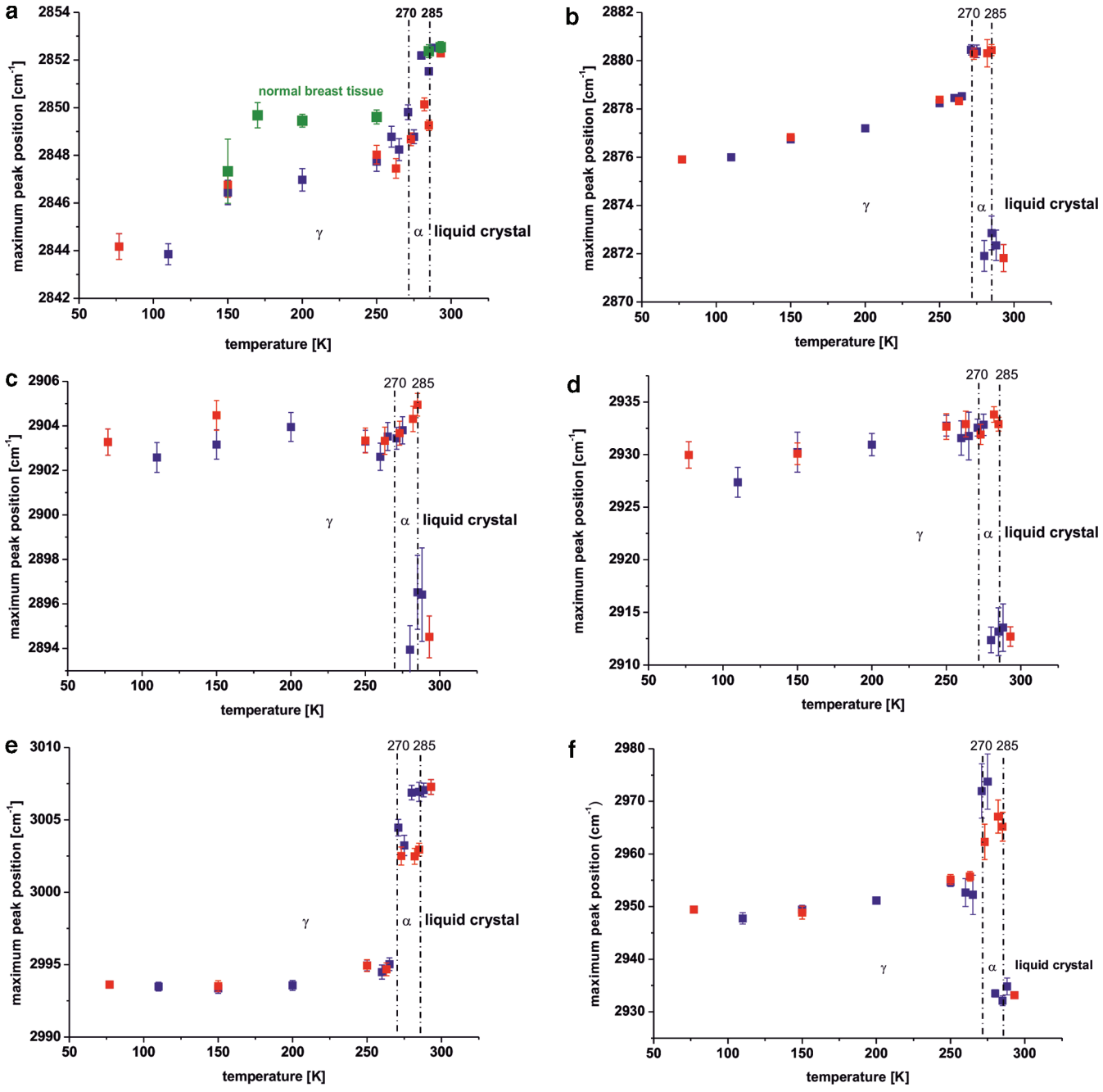

Figure 5. Temperature dependence of the maximum peak positions of oleic acid and the normal breast tissue: (a) $\nu_s(CH_2)$, (b) $\nu_{as}(CH_2)$, (c) $\nu(CH_2)$, (d) $\nu_{as}(CH_2)$ stretching modes, (e) $\nu(=C-H)$, (f) $\nu_{as}(CH_3)$, (red square) heating, (blue square) cooling of the oleic acid, (green square) normal breast tissue.

transitions. The transition at 285 K corresponds to liquid crystal −solid α phase transition. The transition at 270 K has been assigned to the solid α−solid γ transition.

It is interesting that the temperature-dependent plot of the maximum peak positions of the normal breast tissue (Figure 5a) reveals similar phase transitions at identical temperatures, indicating that the oleic acid as the main component of the adipose cells in the normal human breast tissue behaves like the oleic acid in a pure state.

In the view of the results presented so far one can state that evidence has been provided that the oleic acid exists as a separate phase within the human breast tissue. The results appear to suggest that the oleic acid exists as a liquid within the normal breast tissue structure at room temperatures in contrast to the ordered phases of lipids like dipalmitoyl D-α-phosphatidylcholine (DPPC), which is one of the main components of the biomembranes. It has been suggested[18] that the coexistence of the fluid oleic acid and the other ordered lipid membrane phases leads to the enhanced transport of polar molecules across the biomembranes. Briefly, this mechanism can be explained by the formation of permeable interfacial defects within the bilayers of the biomembranes, which is presented in Scheme 1. The hypothesis of ref 18 is related to the phase separation within stratum corneum, but our results presented in this paper seem to

dx.doi.org/10.1021/jm200180f |J. Med. Chem. 2011, 54, 3386–3392

suggest that the same mechanism works within a human breast tissue. It is possible that the phase separation of lipids within the breast tissue may be one of the primary factors in mechanisms of carcinogenesis. Indeed, from detailed inspection, the lipid profile in Figure 2a in the region of the hydrocarbon chains between 2600 and 3200 cm^{-1} of the cancerous breast tissue differs markedly from that of the noncancerous tissue.

It is worth emphasizing that the vibrational properties of water in the region 3200−3800 cm^{-1} for the noncancerous and cancerous breast tissue also differ markedly. Figure 6 shows the Raman images and the Raman spectra of the bulk water for noncancerous and cancerous breast tissues. The colors in Figure 6a and Figure 6b have identical meaning as in Figure 2b and Figure 2c.

First, the Raman spectra presented in Figure 6c evidently show that the breast structure of the noncancerous tissue contains significantly lower levels of hydration than the cancerous tissue. Indeed, the intensity of the OH stretching mode of water is significantly weaker for the normal tissue than that for the cancerous tissue. This observation, analyzed in the context of higher content of adipose cells in normal tissue than in cancerous tissue demonstrated in the Raman imaging by the blue color in Figure 2b and Figure 2c, suggests that the negligible signal of water in the noncancerous breast tissue is related to the hydrophobic nature of adipose tissue. This explanation may rationalize the higher hydration of the cancerous tissue compared to that of the noncancerous tissue demonstrated evidently in Figure 6c. The higher water content in cancerous tissue has also been reported in other organs by optical spectroscopy.[19−21] Although mechanisms that transform the normal tissue into a cancerous are largely unknown, there is growing evidence, based on the study of genes that are overexpressed in cancers, of links between carcinogenesis and cell hydration.[22]

Given the likely existence of separate liquid phase of the oleic acid and the solid phases of membrane lipids within the breast tissue, our results demonstrate that there is a direct link between the amount of oleic acid in breast tissue and hydration of the tissue. Moreover, our recent reports[23−25] demonstrate that there is a correlation between distribution of carotenoids and oleic acid in adipose breast tissue. The results suggest that fatty acids act as a dynamic reservoir that can supply carotenoids to the human organs. Several physiological functions have been attributed to carotenoids. First, carotenoids up-regulate gap junctional communication (GJC) in connexins,[26,27] which plays an important role in exchange of nutrients and ions between connected cells, transfer of electrical signals, and pathways for signaling compounds. It has been speculated that GJC might play a role in carcinogenesis.[26] There is growing evidence that the gap junctions play a role in the regulation of morphogenesis, cell differentiation, secretion of hormones, and growth[28] and in human diseases including human breast cancer.[29]

Scheme 1. Structural Formula of Oleic Acid (a) and Model Representation of Biological Membrane (b)

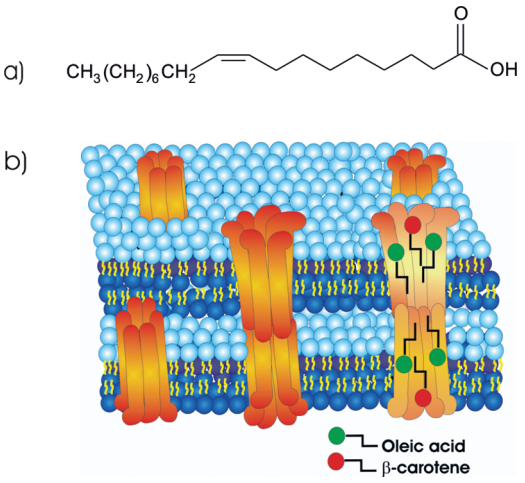

CONCLUSIONS

The paper has illustrated important aspects of the phase transitions of the oleic acid in the pure state and the human breast tissue by Raman studies. The essential findings can be summarized as follows:

(1) Raman spectra and Raman images are sensitive indicators of distribution of lipids in breast tissue structure.
(2) Raman images show that normal breast tissue contains fatty acids in adipose tissue filling the spaces around the lobules and ducts and the fatty acids that make up the cell membrane and nuclear membrane.
(3) Raman spectra are sensitive indicators of phase transitions occurring in the pure state compounds and in the compounds of the breast tissue structure.

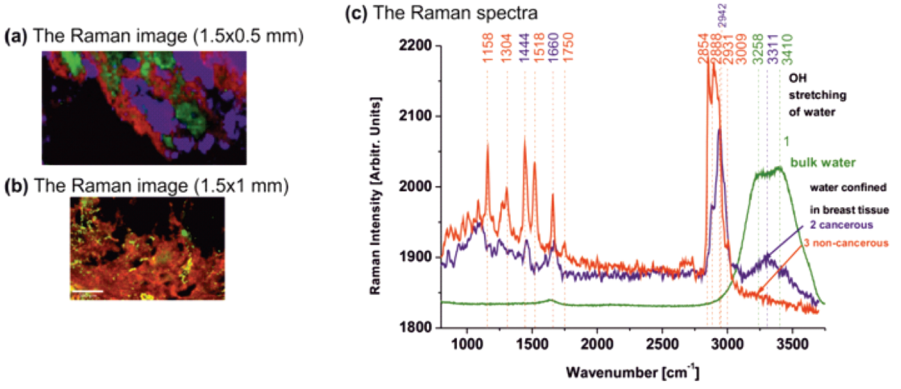

Figure 6. Raman imaging of noncancerous (a) and cancerous breast tissues (infiltrating ductal cancer) (b). Comparison between the Raman spectra of the OH stretching vibrations of water in bulk water (1), cancerous (2) (infiltrating ductal cancer), and noncancerous (3) human breast tissues of the same patient (c).

dx.doi.org/10.1021/jm200180f |J. Med. Chem. 2011, 54, 3386–3392

(4) The liquid−solid α phase and the solid α−γ transition have been identified in the pure state of the oleic acid and the oleic acid contained in the breast tissue.
(5) The OH stretching vibrations of water can be useful as potential Raman biomarkers to distinguish between the cancerous and the noncancerous human breast tissues. We have found that water amount confined in the cancerous tissue is markedly different from that in the noncancerous tissue.
(6) Our results provide experimental evidence for the role played by the lipid profile and cell hydration as factors of particular significance in differentiation of the noncancerous and cancerous breast tissues.

EXPERIMENTAL SECTION

Sample Preparation. Oleic acid was purchased from Sigma Aldrich (product no. O1008) and used without purification. The chemical structure of oleic acid and the model representation of the biological membrane are depicted in Scheme 1.

Patients and Samples. We have studied ex vivo noncancerous and cancerous (infiltrating ductal carcinoma) samples of fresh human breast tissues. All procedures were conducted under a protocol approved by the Bioethic Committee at the Medical University of Lodz (RNNj30j11jKE/15/02/2011). The tissue sample from the tumor mass and the tissue from the safety margins outside the tumor mass were cryosectioned with a microtome into 2 μm thick sections for histopathological and Raman analysis. The histological analysis was performed by pathologists from the Medical University of Lodz, Department of Pathology, Chair of Oncology. The use of the samples for research did not affect the course of the operation or treatment of the patients. The thin sections of 2 μm layers (without staining) have been examined by Raman imaging. The adjacent thin sections of the samples were stained with hematoxylin and eosin to permit histological examination of the suspected areas. The samples were not prepared by the paraffin-embedding procedure because the wax has its own vibrational spectra of lipids that overlap those from the breast tissue, while deparafinization removes the fatty acids that are the indicators of cancer pathology. The samples were also examined by Raman spectroscopy in the temperature range of 293−77 K. The fresh tissue samples were measured without any fixation in formalin to avoid alteration of the tissue.

DSC. Calorimetric data were obtained with a differential scanning calorimeter DSC TA Instruments Q 200, which has temperature accuracy of ±0.1 °C, temperature precision of ±0.05 °C, calorimetric precision (based on metal standards) of ±0.1%, maximum calorimetric sensitivity of 0.2 μW, sensitivity/resolution of ≥30 mW/°C, and dynamic range of ±500 mW.

Raman Spectroscopy (293−77 K). Raman spectra were recorded with Ramanor U1000 (JobinYvon) and Spectra Physics 2017-04S argon ion laser operating at 514 nm. The samples were placed in the cryostat (Oxford Instruments Limited) and commercial glass ampules mounted in a special cell arrangement. The samples were introduced as a liquid, and they were cooled in the cryostat equipped with a heater and thermocouples for temperature monitoring. Cooling of the sample was achieved by the use of a 50 L Dewar which supplied a stream of liquid nitrogen through a vacuum jacketed tube to the cryostat coat. In order to ensure that the equilibrium phases are generated, the samples were cooled slowly (0.5 K/min).

Raman Imaging. All Raman images reported here were acquired using Alpha 500 RA (WITec, Ulm, Germany) model consisting of an Olympus microscope coupled with an UHTS spectrometer and a Newton-CCD camera operating in standard mode with 1024 × 127 pixels at −64 °C with full vertical binning. The second harmonic (532 nm) of a neodymium yttrium aluminum garnet (Nd:YAG) laser is focused on the sample with a 50× objective with a numerical aperture NA of 0.50 to the spot of 200 nm. The average laser excitation power was 10 mW. Before recording of the Raman image, the fluorescence in the sample was quenched by illumination at each point with the excitation light during 500 ms. The quenching of the fluorescence was very effective because of the high optical density provided by the light focusing.

The 2D array images of individual Raman spectra contained in each pixel were evaluated by the basis analysis method. In this data analysis method each measured Raman spectrum of the 2D spectral array is compared to the basis spectra by using a least-squares fit. Such basis spectra are created from the average spectra of three different areas in the sample. The weight factor in each point is represented as a 2D image of the corresponding color and mixed coloring component.

AUTHOR INFORMATION

Corresponding Author

*Telephone: +48 42 6313175 and +48 42 6313188. Fax: +48 42 684-00-43. E-mail: abramczy@mitr.p.lodz.pl.

ACKNOWLEDGMENT

This project has been funded by the National Science Centre (Grant 2940/B/T02/2011/40). We also gratefully acknowledge the support of this work through the Grant 3845/B/T02/2009/37 and the Dz. St 2011.

ABBREVIATIONS USED

DSC, differential scanning calorimetry; Her-2/neu, human epidermal growth factor receptor 2; DPPC, dipalmitoyl D-α-phosphatidylcholine; GJC, gap junctional communication; UHTS, ultrahigh transmission spectrometer; Nd:YAG, neodymium yttrium aluminum garnet

REFERENCES

(1) Mamalakis, G.; Hatzis, C.; de Bree, E.; Sanidas, E.; Tsiftsis, D. D.; Askoxylakis, J.; Daskalakis, M.; Tsibinos, G.; Kafatos, A. Adipose tissue fatty acids in breast cancer patients versus healthy control women from Crete. *Ann. Nutr. Metab.* **2009**, *54*, 275–282.

(2) Menendez, J. A.; Vellon, L.; Colomer, R.; Lupu, R. Oleic acid, the main monounsaturated fatty acid of olive oil, suppresses Her-2/neu (erb B-2) expression and synergistically enhances the growth inhibitory effects of trastuzumab (Herceptine) in breast cancer cells with Her-2/neu oncogene amplification. *Ann. Oncol.* **2005**, *16*, 359–371.

(3) Soto-Guzman, A.; Navarro-Tito, N.; Castro-Sanchez, L.; Martinez-Orozco, R.; Salazar, E. P. Oleic acid promotes MMP-9 secretion and invasion in breast cancer cells. *Clin. Exp. Metastasis* **2010**, *27*, 505–515.

(4) Navarro-Tito, N.; Soto-Guzman, A.; Castro-Sanchez, L.; Martinez-Orozco, R.; Salazar, E. P. Oleic acid promotes migration on MDA-MB-231 breast cancer cells through an arachidonic acid-dependent pathway. *Int. J. Biochem. Cell Biol.* **2010**, *42*, 306–317.

(5) Iwahashi, M.; Yamaguchi, Y.; Kato, T.; Horiuchi, T.; Sakurai, I.; Suzuki, M. Temperature dependence of molecular conformation and liquid structure of *cis*-9-octadecenoic acid. *J. Phys. Chem.* **1991**, *95*, 445–451.

(6) Iwahashi, M.; Hachiya, N.; Hayashi, Y.; Matsuzawa, H.; Suzuki, M.; Fujimoto, Y.; Ozaki, Y. Dissociation of dimeric *cis*-9-octadecenoic acid in its pure liquid state as observed by near-infrared spectroscopic measurement. *J. Phys. Chem.* **1993**, *97*, 3129–3133.

(7) Iwahashi, M.; Kasahara, Y.; Matsuzawa, H.; Yagi, K.; Nomura, K.; Terauchi, H.; Ozaki, Y.; Suzuki, M. Self-diffusion, dynamical molecular conformation, and liquid structures of *n*-saturated and unsaturated fatty acids. *J. Phys. Chem.* **2000**, *104*, 6186–6194.

(8) Kaneko, F.; Yano, J.; Sato, K. Diversity in the fatty-acid conformation and chain packing of *cis*-unsaturated lipids. *Curr. Opin. Struct. Biol.* **1998**, *8*, 417–425.
(9) Kaneko, F.; Yamazaki, K.; Kitagawa, K.; Kikyo, T.; Kobayashi, M.; Kitagawa, Y.; Matsuura, Y.; Sato, K.; Suzuki, M. Structure and crystallization behavior of the β phase of oleic acid of outstanding interest. *J. Phys. Chem.* **1997**, *101*, 1803–1809.
(10) Abrahamsson, S.; Dahlen, B.; Lofgren, H.; Pascher, J. Lateral packing of hydrocarbon chains. *Prog. Chem. Fats Other Lipids* **1978**, *16*, 125–143.
(11) Kaneko, F.; Tashiro, K.; Kobayashi, M. Polymorphic transformations during crystallization processes of fatty acids studied with FT-IR spectroscopy. *J. Cryst. Growth* **1999**, *198*−*199*, 1352–1359.
(12) Kobayashi, M.; Kaneko, F.; Sato, K.; Suzuki, M. Vibrational spectroscopic study on polymorphism and order−disorder phase transition in oleic acid. *J. Phys. Chem.* **1986**, *90*, 6371–6378.
(13) Verma, S. P.; Wallach, D. F. H. Raman spectra of some saturated, unsaturated and deuterated C18 fatty acids in the HCH-deformation and CH-stretching regions. *Biochem. Biophys. Acta* **1977**, *486*, 217–227.
(14) Kim, Y.; Strauss, H. L.; Snyder, R. G. Raman evidence for premelting in the .alpha. and .beta. phases of oleic acid. *J. Phys. Chem.* **1988**, *92*, 5080–5082.
(15) Tandon, P.; Forster, G.; Neubert, R.; Wartewig, S. Phase transitions in oleic acid as studied by X-ray diffraction and FT-Raman spectroscopy. *J. Mol. Struct.* **2000**, *524*, 201–215.
(16) Hiramatsu, N.; Inoue, T.; Suzuki, M.; Sato, K. Pressure study on thermal transitions of oleic acid polymorphs by high-pressure differential thermal analysis. *Chem. Phys. Lipids* **1989**, *51*, 47–53.
(17) Palmer, G.; Zhu, C.; Breslin, T.; Xu, F.; Gilchrist, K.; Ramanujam, N. Comparison of multiexcitation fluorescence and diffuse reflectancy spectroscopy for the diagnosis of breast cancer. *IEEE Trans. Biomed. Eng.* **2003**, *50*, 1233–1242.
(18) Ongpipattanakul, B.; Burnette, R. R.; Potts, R. O.; Francoeur, M. L. Evidence that oleic acid exists in a separate phase within stratum corneum lipids. *Pharm. Res.* **1991**, *8*, 350–354.
(19) Mo, J.; Zheng, W.; Low, J. J. H.; Ng, J.; Ilancheran, A.; Huang, Z. High wavenumber Raman spectroscopy for in vivo detection of cervical dysplasia. *Anal. Chem.* **2009**, *81*, 8908–8915.
(20) Hornung, R.; Pham, T. H.; Keefe, K. A.; Berns, M. W.; Tadir, Y.; Tromberg, B. J. Quantitative near-infrared spectroscopy of cervical dysplasia *in vivo*. *Hum. Reprod.* **1999**, *14*, 2908–2916.
(21) Kondepati, V.; Heise, H.; Backhaus, J. J. Recent applications of near-infrared spectroscopy in cancer diagnosis and therapy. *Anal. Bioanal. Chem.* **2008**, *390*, 125–139.
(22) McIntyre, G. I. Cell hydration as the primary factor in carcinogenesis: a unifying concept. *Med. Hypotheses* **2006**, *66*, 518–526.
(23) Abramczyk, H.; Surmacki, J.; Brożek-Płuska, B.; Morawiec, Z.; Tazbir, M. The hallmarks of breast cancer by Raman spectroscopy. *J. Mol. Struct.* **2009**, *924*−*926*, 175–182.
(24) Abramczyk, H.; Placek, I.; Brożek-Płuska, B.; Kurczewski, K.; Morawiec, Z.; Tazbir, M. Human breast tissue cancer diagnosis by Raman spectroscopy. *Spectroscopy* **2008**, *22*, 113–121.
(25) Brożek-Płuska, B.; Placek, I.; Kurczewski, K.; Morawiec, Z.; Tazbir, M.; Abramczyk, H. Breast cancer diagnostics by Raman spectroscopy. *J. Mol. Liq.* **2008**, *141*, 145–148.
(26) Lee, S. W.; Tomasetto, C.; Paul, D.; Keyomarsi, K.; Sager, R. J. Transcriptional downregulation of gap-junction proteins blocks junctional communication in human mammary tumor cell lines. *Cell Biol.* **1992**, *188*, 1213–1221.
(27) Yeum, K. J.; Ahn, S. H.; Rupp de Paiva, S. A.; Lee-Kim, Y. Ch.; Krinsky, N. I.; Russell, R. M. Correlation between carotenoid concentrations in serum and normal breast adipose tissue of women with benign breast tumor or breast cancer. *J. Nutr.* **1998**, *1*−*4*, 1920–1926.
(28) Bertram, J. S. Induction of connexin 43 by carotenoids: functional consequences. *Arch. Biochem. Biophys.* **2004**, *430*, 120–126.
(29) Kumar, N. M.; Gilula, N. B. The gap junction communication channel. *Cell* **1996**, *84*, 381–388.
(30) Misra, R. M.; Jain, A.; Tandon, P.; Wartewig, S.; Gupta, V. D. Normal mode analysis of gamma form of oleic acid. *Chem. Phys. Lipids* **2006**, *142*, 70–83.
(31) Parker, F. S. *Applications of Infrared Raman, and Resonance Raman Spectroscopy in Biochemistry*; Plenum Press: New York, 1983; pp 421−480.